

A study of kinetic modelling and reaction pathway of 2,4-dichlorophenol transformation by photo-fenton-like oxidation

W. Chu^{*}, C.Y. Kwan, K.H. Chan, S.K. Kam

Department of Civil and Structural Engineering, Research Centre for Environmental Technology and Management,
The Hong Kong Polytechnic University, Hungghom, Kowloon, Hong Kong

Received 30 November 2004; received in revised form 27 January 2005; accepted 31 January 2005

Available online 21 February 2005

Abstract

The degradation of 2,4-dichlorophenol (2,4-DCP) by the photo-Fenton-like ($\text{Fe}^{3+}/\text{H}_2\text{O}_2/\text{UVC}$) process under various reaction conditions was investigated. It was interesting to find that the reaction kinetics of 2,4-DCP in $\text{Fe}^{3+}/\text{H}_2\text{O}_2/\text{UVC}$ systems varied depending on the initial $[\text{Fe}^{3+}]$ concentration. A pseudo first-order kinetic and a non-conventional kinetic were discovered at low and higher $[\text{Fe}^{3+}]$ concentrations, respectively. A model was used to simulate the non-conventional kinetic process, where two character parameters (the initial decay rate and the final decay fraction) were found to be critical in determining the process. The two parameters successfully quantify the photo-Fenton-like oxidation under different concentrations of $[\text{Fe}^{3+}]$ and $[\text{H}_2\text{O}_2]$ and the corresponding ratios of $\text{Fe(III)}/\text{H}_2\text{O}_2$. The reaction intermediates were identified by an LC/MS analysis and a reaction mechanism was proposed.

© 2005 Elsevier B.V. All rights reserved.

Keywords: 2,4-Dichlorophenol; Fenton; Mechanism; Oxidation; Photo

1. Introduction

2,4-Dichlorophenol (2,4-DCP) is a chemical precursor that contributes principally to the manufacture of a widely used herbicide 2,4-dichlorophenoxy acetic acid (2,4-D). After the herbicides have been applied to agricultural sites, 2,4-DCP is the major transformation product of 2,4-D by solar-photolysis and/or microbial activities in the nearby soil [1] or in natural water [2]. Similarly, upon the exposure of 2,4-D, it is metabolized to 2,4-DCP in bluegill sunfish [3] and in transgenic cotton plants [4]. 2,4-DCP has also been found in disinfected water after chlorination [5], in the incineration flue gas of municipal waste [6], or in pulp and paper effluents [7]. Chlorophenols including 2,4-DCP can be removed by biodegradation [8], adsorption over activated carbon [9], or through papermill sludge [10].

In addition, ultraviolet (UV) irradiation has been shown to degrade chlorophenols [11,12] by promoting them to

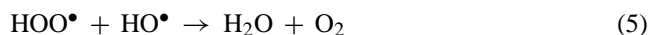
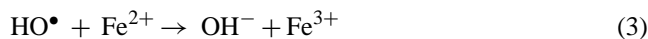
their excited singlet states, which may then deactivate to triplet states through intersystem crossing [13]. Subsequently, three possible pathways that the excited triplets may undergo are homolysis, heterolysis and photoionization [14]. Researchers have shown that combining another source of oxidants (e.g., hydrogen peroxide and/or ozone) with UV can improve the decomposition of the pollutants [15–17]. Recently, Fe^{3+} and H_2O_2 used together with UV irradiation was found to be a more effective process than conventional Fenton oxidation ($\text{Fe}^{2+}/\text{H}_2\text{O}_2$) and equivalent to the photo-Fenton ($\text{Fe}^{2+}/\text{H}_2\text{O}_2/\text{UV}$) process [18]. In the photo-Fenton-like process ($\text{Fe}^{3+}/\text{H}_2\text{O}_2/\text{UVC}$), hydroxyl radicals are generated and will typically attack the organic substrate and form stable and/or mineralized end products [19]:



This new photo-Fenton-like oxidaton usually performs better in acidic aqueous solutions ($\text{pH} < 4$), and has been employed to treat synthetic municipal wastewater [20], textiles

^{*} Corresponding author. Tel.: +852 2766 6075; fax: +852 2334 6389.
E-mail address: cewchu@polyu.edu.hk (W. Chu).

[21,22], and industrial effluents containing pharmaceutical formulations [23], or wood preservatives [24]. However, the process may be hindered if the reaction condition was not properly adjusted [25]. This is because excess oxidants may be detrimental to the overall reaction and not cost-effective because the additional oxidants may act as scavengers by quenching the hydroxyl free radicals, as shown below [7]:



As a result, less reactive HOO^\bullet (hydroperoxyl) radicals may be produced, leading to radical consumptive side-reactions and eventually reducing the overall oxidative capacity. Therefore, it is necessary to fine-tune the process by examining the reaction kinetics (at different concentrations of ferric ion and hydrogen peroxide) and developing a mathematical model to optimize the degradation of 2,4-DCP by $\text{Fe}^{3+}/\text{H}_2\text{O}_2/\text{UVC}$ system for purposes of the design. In addition, the reaction intermediates have been identified in this study and a photooxidation mechanism of 2,4-DCP by photo-Fenton-like oxidaton has been proposed.

2. Materials and methods

2.1. Chemicals

The 2,4-dichlorophenol (2,4-DCP) is a colorless crystal at room temperature and has a strong characteristic odour. Non-labelled 2,4-DCP of 99% purity was purchased from Riedel-de Haen. Acetonitrile and methanol were HPLC grade and obtained from Lab-Scan. Ferric sulphate hydrate and 30% hydrogen peroxide were purchased from Riedel-de Haen and British Drug Houses (BDH), respectively. Sulfuric acid and diluted sodium hydroxide were used to adjust the initial pH of the solutions.

2.2. Experimental procedures

In a direct photolysis process, 25 mL of 3.06 mM 2,4-DCP was mixed with 175 mL deionized water in a 400 mL quartz column, and the pH level of the mixture was adjusted to 3. The reaction was carried out in an RPR-200 RayonetTM photochemical reactor equipped with a magnetic stirrer and a cooling fan, as shown in Fig. 1. The light sources were four 253.7 nm (wavelengths < 280 nm, is known as UVC) phosphor-coated low-pressure mercury lamps that were equally spaced inside the reactor so that the ultraviolet light could pass through the mixture more homogeneously. The UV-lamps were turned on 15 min before the reaction

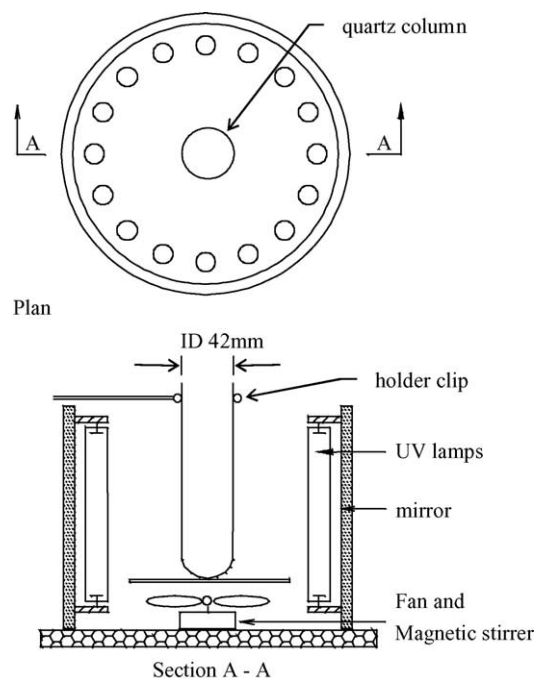


Fig. 1. The plan and sectional views of the RPR-200 Rayonet photochemical reactor.

started for a steady-state operation. After the reaction was started (by placing the quartz column into the reactor), 1 mL of the sample was withdrawn from the quartz column at pre-selected time intervals.

In the $\text{Fe}^{3+}/\text{H}_2\text{O}_2/\text{UVC}$ process, the initial concentrations of Fe^{3+} were set at 0.1, 0.2, 0.3, and 0.4 mM; and five different Fe^{3+} to H_2O_2 molar ratios (i.e., $\text{Fe(III)}/\text{H}_2\text{O}_2$) at 0.20, 0.33, 0.50, 1.00, and 2.00 were chosen to conduct the tests. After mixing all of the solutions together (except the H_2O_2) with the right portion in the quartz column, the solution pH was adjusted to around 3 and the reaction was then initiated by adding a H_2O_2 solution and simultaneously switching on the UV-lamps. One millilitre of solution was pipetted out from the quartz column and then mixed with the same amount of methanol to quench the reaction.

2.3. Instrumental analysis

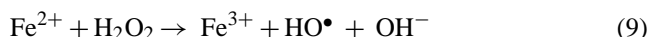
Each illuminated sample was quantified by LC equipped with a Restek column packed with pinnacle octyl amine ($5 \mu\text{m}$, $0.46 \text{ cm} \times 25 \text{ cm}$). The mobile phase was a mixture of acetonitrile and 0.15% of acetic acid at a ratio of 50:50. A Finnigan LCQTM DUO ion trap mass spectrometer coupled to the LC was employed to identify the intermediates. The electrospray ionization (ESI) source was operated in a negative mode. A linear gradient of 0.15% of acetic acid and acetonitrile that was increased from a ratio of 100:0 to 50:50 in 35 min at a flow rate of 1.0 mL/min was used to separate the 2,4-DCP and the intermediates.

3. Results and discussion

3.1. Direct photolysis and photo-Fenton-alike oxidation of 2,4-DCP

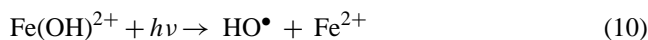
The degradation of 0.38 mM 2,4-DCP by direct photolysis in water was conducted as a blank compared to that of a specific photo-Fenton-like oxidation at 0.1 mM Fe^{3+} and 0.05 mM H_2O_2 (i.e., $\text{Fe(III)/H}_2\text{O}_2 = 2.00$). In general, pseudo first-order kinetics were observed for both of the cases, so the plot of [2,4-DCP] the decay fractions in $\ln(C/C_0)$ versus the reaction time (t) resulted in a linear relationship (see Fig. 2(a)). The rate constants of the dark Fenton-like ($\text{Fe}^{3+}/\text{H}_2\text{O}_2$), direct photolysis and the photo-Fenton-like oxidation were 2×10^{-5} , 1×10^{-4} and $5 \times 10^{-4} \text{ s}^{-1}$, respectively, which indicated that the photodecay rate could be improved five times with the aid of Fe^{3+} and H_2O_2 upon UV irradiation. Since the dark Fenton-like system was relatively minor, its contribution could be negligible. Consequently, further, experiments were performed by increasing the dose of H_2O_2 at the same $\text{Fe(III)/H}_2\text{O}_2$ ratio to study whether any further enhancement in the reaction rate was possible. At a fixed $[\text{Fe}^{3+}]$, the $\text{Fe(III)/H}_2\text{O}_2$ ratios were adjusted to 1.00,

0.50, and 0.33 by increasing the concentration of $[\text{H}_2\text{O}_2]$ to two, four, and six times, respectively, compared to the original condition. The resulting natural logarithms of the 2,4-DCP decay fractions are presented in Fig. 2(b). Similarly, these reactions also followed the pseudo first-order kinetics; and the rate constants for the $\text{Fe(III)/H}_2\text{O}_2$ ratios of 1.00, 0.50, and 0.33 were $6 \times 10^{-4} \text{ s}^{-1}$, $7 \times 10^{-4} \text{ s}^{-1}$ and $9 \times 10^{-4} \text{ s}^{-1}$, respectively. Both the initial rate and the final removal fraction increased as $\text{Fe(III)/H}_2\text{O}_2$ ratio decreased, implying that a higher level of $[\text{H}_2\text{O}_2]$ could efficiently improve the degradation of 2,4-DCP. This is likely due to higher yields of the hydroxyl radical (HO^\bullet) via both the higher cleavage of the H_2O_2 induced by UV (Eq. (8)) and the participation of Fenton's reaction (Eq. (9)).



Since no rate retardation was observed within the tested ranges, the doses of H_2O_2 selected were within the optimum range without causing the futile consumption of hydroxyl radicals in the solution.

Another way to introduce significant effects on the reaction is to regulate the concentration of Fe^{3+} . The variations in the level of $[\text{Fe}^{3+}]$ in the $\text{Fe}^{3+}/\text{H}_2\text{O}_2/\text{UVC}$ system were therefore investigated. When the concentration of $[\text{Fe}^{3+}]$ was increased from 0.1 to 0.2 mM, the transformation of 2,4-DCP improved significantly at all $\text{Fe(III)/H}_2\text{O}_2$ ratios, but these reactions no longer followed the pseudo first-order kinetics in accordance with the rate law (see Fig. 2(c)). It was noticed that the reaction could be divided into two stages, with a rapid initial stage followed by a stagnant stage. In general, the lower the $\text{Fe(III)/H}_2\text{O}_2$ ratios the faster the decay rate in the initial stage and the higher 2,4-DCP decay fractions in the stagnant stage. Theoretically, in the absence of other chelating ligands in the solution, Fe^{3+} coordinates with water molecules to form complexes $[\text{Fe}(\text{H}_2\text{O})_6]^{3+}$, $[\text{Fe}(\text{OH})]^{2+}$, $[\text{Fe}(\text{OH})_2]^+$, and $[\text{Fe}_2(\text{OH})_2]^{4+}$, where $[\text{Fe}(\text{OH})]^{2+}$ is predominant among the four Fe^{III} -hydroxy complexes at $\text{pH} \approx 3$ [26]. The photoreduction of $\text{Fe}(\text{OH})^{2+}$ yields a hydroxyl radical (HO^\bullet) and a ferrous ion (Eq. (10)). The former can be used to directly oxidize 2,4-DCP, while the latter can, further, react with H_2O_2 in the solution (via Fenton's process) to generate additional hydroxyl radicals as indicated before in Eq. (9):



The stagnant stage indicates that one or more of the active reagents (such as hydrogen peroxide and/or $\text{Fe}(\text{OH})^{2+}$) is approaching the level of depletion. After all of the available hydroxyl radicals in the solution have been exhausted, direct UV-photolysis might become the single (but ineffective) pathway to degrade 2,4-DCP. Besides, the accumulation of intermediates may be also responsible for the tailing of the 2,4-DCP decay curve because many other daughter compounds will consume and/or compete for the hydroxyl radicals. This can be justified by the oxidative intermediates

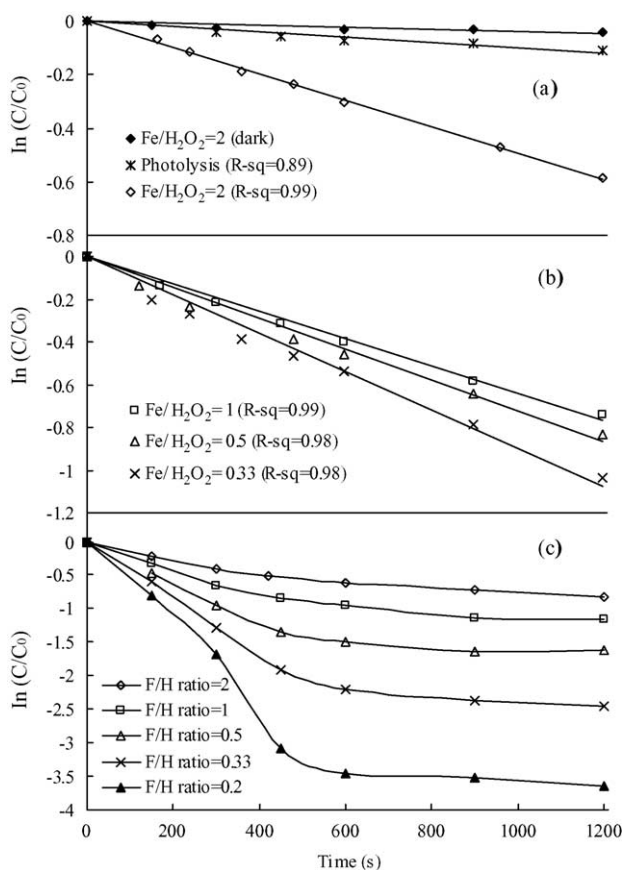


Fig. 2. The pseudo first-order degradation of 2,4-DCP by direct photolysis and photo-Fenton-like oxidation at 253.7 nm at $\text{pH} \approx 3$. The initial $[\text{Fe}^{3+}]$: (a) 0.1 mM, (b) 0.1 mM, and (c) 0.2 mM with various $\text{Fe(III)/H}_2\text{O}_2$ ratios. R^2 is the regression coefficients of the linear plots.

that have been identified in the LC/MS analysis (to be discussed later in the section on the reaction mechanism).

The two-stage phenomenon was reconfirmed by elevating the concentration of Fe^{3+} to 0.3 and 0.4 mM, while keeping the $\text{Fe(III)/H}_2\text{O}_2$ ratios at 0.20, 0.33, 0.50, 1.00, and 2.00, in which analogous trends with higher reaction rates were observed. A satisfactory result was obtained when 2,4-DCP was 100% degraded (to a non-detectable level) by photo-Fenton-like oxidation in 600 s, as the $[\text{Fe}^{3+}]$ and $\text{Fe(III)/H}_2\text{O}_2$ were at 0.4 mM and 0.33, respectively. Since the reaction conditions to completely transform 2,4-DCP have been identified, a further increase in the concentrations of Fe^{3+} and H_2O_2 would not be necessary. Based on the collected data, a mathematic model can be developed to estimate the required performances based on the selected reaction conditions, so that better cost-effectiveness can be achieved.

3.2. Model development

The oxidation of 2,4-DCP by low $[\text{Fe}^{3+}]$ concentrations can generally be easily described by simple pseudo first-order kinetics. Because these reaction conditions have less value in real applications, the model derivation will focus on more complicated conditions with higher $[\text{Fe}^{3+}]$ concentrations at various $\text{Fe(III)/H}_2\text{O}_2$ ratios. Under these circumstances, the photo-Fenton-like process is composed of a fast initial stage, followed by a stagnant stage with a declining reaction rate. This process can be described by a two-stage model that was previously proposed by Chan and Chu [27] where $\text{Fe}^{3+}/\text{H}_2\text{O}_2$ ratio > 0 :

$$\frac{[2,4\text{-DCP}]}{[2,4\text{-DCP}]_0} = 1 - \frac{t}{\rho + \sigma t} \quad (11)$$

where $[2,4\text{-DCP}]$ is the concentration of 2,4-DCP remaining in the solution at time t (s), $[2,4\text{-DCP}]_0$ is the initial concentration at time zero, ρ (s) and σ (dimensionless) are the two important constants relating to the decay rate and the remaining 2,4-DCP in photo-Fenton-like process, respectively. As the time is equal to zero, the above equation can be rearranged as:

$$\frac{d([2,4\text{-DCP}]/[2,4\text{-DCP}]_0)}{dt} = -\frac{1}{\rho} (\text{sec}^{-1}) \quad (12)$$

where $1/\rho$ is the initial slope of the decay curve that is directly proportional to the initial decay rate of the reaction. However, when the time is approaching infinity, the term ρ can be neglected compared to the term σt , and Eq. (11) can be solved in terms of σ :

$$\frac{1}{\sigma_\infty} = 1 - \frac{[2,4\text{-DCP}]_{t \rightarrow \infty}}{[2,4\text{-DCP}]_0} \quad (13)$$

The physical meaning of $1/\sigma$ is the final decay fraction (FDF) of 2,4-DCP in $\text{Fe}^{3+}/\text{H}_2\text{O}_2/\text{UVC}$ system. To solve these two constants, Eq. (11) can be linearized to:

$$\frac{t}{1 - ([2,4\text{-DCP}]/[2,4\text{-DCP}]_0)} = \rho + \sigma t \quad (14)$$

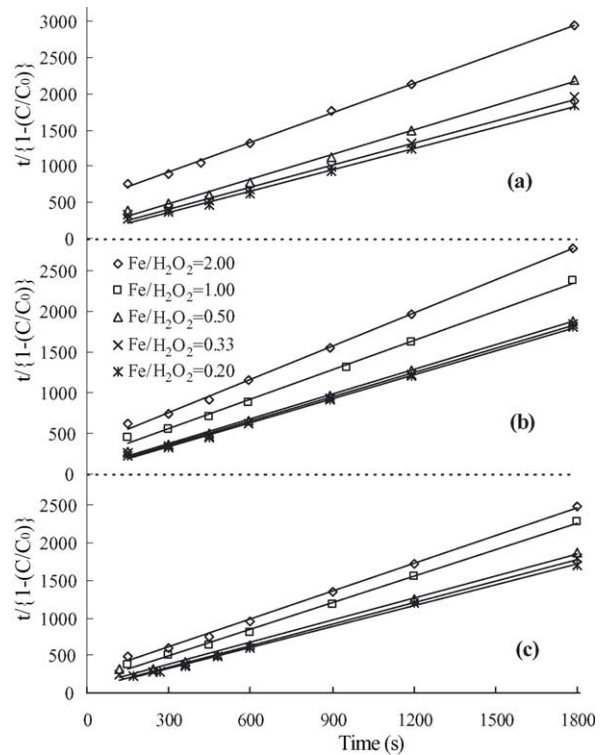


Fig. 3. Linear relationship of $t/\{1-(C/C_0)\}$ with time at various $\text{Fe(III)/H}_2\text{O}_2$ ratios and with the initial $[\text{Fe}^{3+}]$: (a) 0.2 mM, (b) 0.3 mM, and (c) 0.4 mM.

Fig. 3 shows the plots of $t/(1-[2,4\text{-DCP}]/[2,4\text{-DCP}]_0)$ versus t at $[\text{Fe}^{3+}]$ concentrations of 0.2, 0.3, 0.4 mM at various $\text{Fe(III)/H}_2\text{O}_2$ ratios (2.0 to 0.2). The values of ρ and σ under different conditions can be obtained from the intercepts and slopes of the linear curves, respectively. After a run of analysis, the values of ρ (the reciprocal form of the initial rate) were found to have a good linear relationship with the corresponding $\text{Fe(III)/H}_2\text{O}_2$ ratios (as shown in Fig. 4), where the lower the ratio, the lower the ρ (or the higher the initial decay rate $1/\rho$). The results show that at a given concentration of Fe^{3+} , the increase in the initial dose of H_2O_2 can accelerate

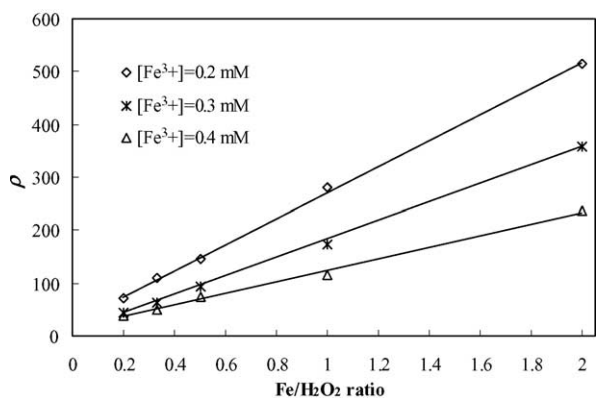


Fig. 4. Effect of $\text{Fe(III)/H}_2\text{O}_2$ ratio on the values of ρ at different $[\text{Fe}^{3+}]$ levels.

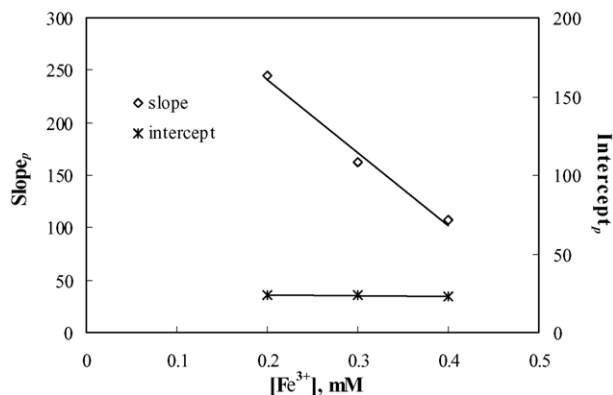


Fig. 5. Correlations of slope_ρ and intercept_ρ with the initial concentrations of Fe³⁺.

the initial decay of 2,4-DCP. To cross-check the effect of the Fe³⁺ concentration on the same issue, Fig. 4 was, further, analyzed as shown in Fig. 5, where the concentration of Fe³⁺ is interrelated to the values of the slope (slope_ρ) and intercept (intercept_ρ) that were determined from Fig. 4 with the following equations:

$$\text{Slope}_\rho = 310 - 69.1 \times [\text{Fe}^{3+}] \quad (15)$$

$$\text{Intercept}_\rho = 25 - 0.5 \times [\text{Fe}^{3+}] \quad (16)$$

As the initial concentration of [Fe³⁺] increased, referring to the declining slopes_ρ and intercept_ρ from the above equations, the general tendency of the resulting ρ decreased as well. This suggests that the initial rate of the 2,4-DCP decay (i.e., 1/ρ) is also simultaneously dominated by the initial concentration of Fe³⁺.

However, it should be noted that the intercept_ρ in Fig. 4 carries an important feature in the photo-Fenton-like oxidation. It represents the maximum initial rate that can theoretically be achieved as the Fe(III)/H₂O₂ ratio approaches zero (or the [H₂O₂] will be in excess). It can be seen that all of the curves in Fig. 4 have similar intercepts (as also shown in Eq. (16), the intercept_ρ varies from 25.1 to 25.2 in the tested

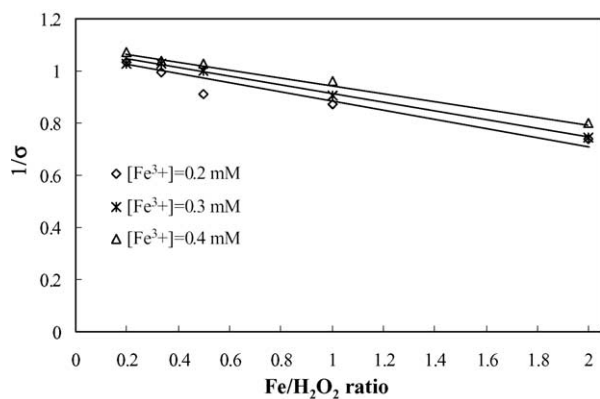


Fig. 6. Linear relationship of 1/σ and the Fe(III)/H₂O₂ ratio at different [Fe³⁺] levels.

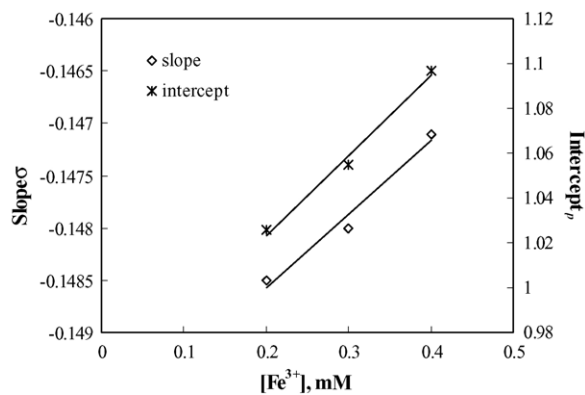


Fig. 7. Relationship of [Fe³⁺] with 1/σ in terms of slope_{1/σ} and intercept_{1/σ}.

ranges) regardless of the initial concentration of Fe³⁺. This is reasonable, because when there is an overdose of [H₂O₂], the contributions become minor as a result of [Fe³⁺] or the Fe(III)/H₂O₂ ratio.

In addition to the initial rate (1/ρ), the FDF (1/σ) is another critical factor that can be used to quantify the 2,4-DCP degradation. The analysis between 1/σ and the Fe(III)/H₂O₂ ratio is illustrated in Fig. 6. The negative slope indicates that the FDF reduces as either the Fe(III)/H₂O₂ ratio or [Fe³⁺] concentration increases. By using the slope_{1/σ} and intercept_{1/σ} of the FDF obtained in Fig. 6, their correlations with [Fe³⁺] are demonstrated in Fig. 7 with the following linear equations:

$$\text{Slope}_{1/\sigma} = -0.1493 + 0.0007 \times [\text{Fe}^{3+}] \quad (17)$$

$$\text{Intercept}_{1/\sigma} = 0.9877 + 0.0368 \times [\text{Fe}^{3+}] \quad (18)$$

The products of the slope and the [Fe³⁺] of the first term on the right-hand side of both of the equations are relatively small, compared with the absolute number of corresponding intercepts (the second term from the right). This suggests that the [Fe³⁺] is likely to be insignificant in determining the FDF, while the [H₂O₂] should be the dominant reactant in determining the removal efficiency of 2,4-DCP by the photo-Fenton-like oxidation. Therefore, an efficient way to improve

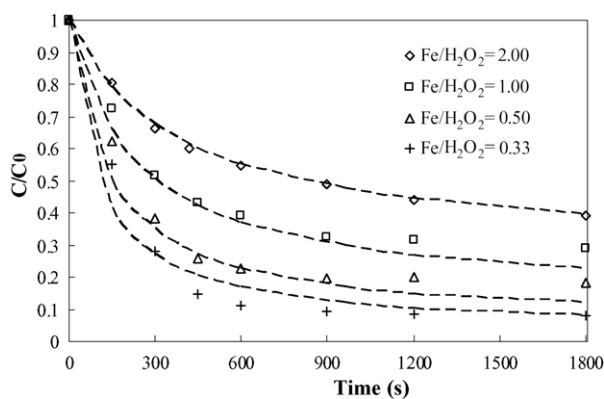


Fig. 8. Comparison of the experimental data (symbols) with the model calculation (dashed lines) at [Fe³⁺] = 0.2 mM at various Fe(III)/H₂O₂ ratios.

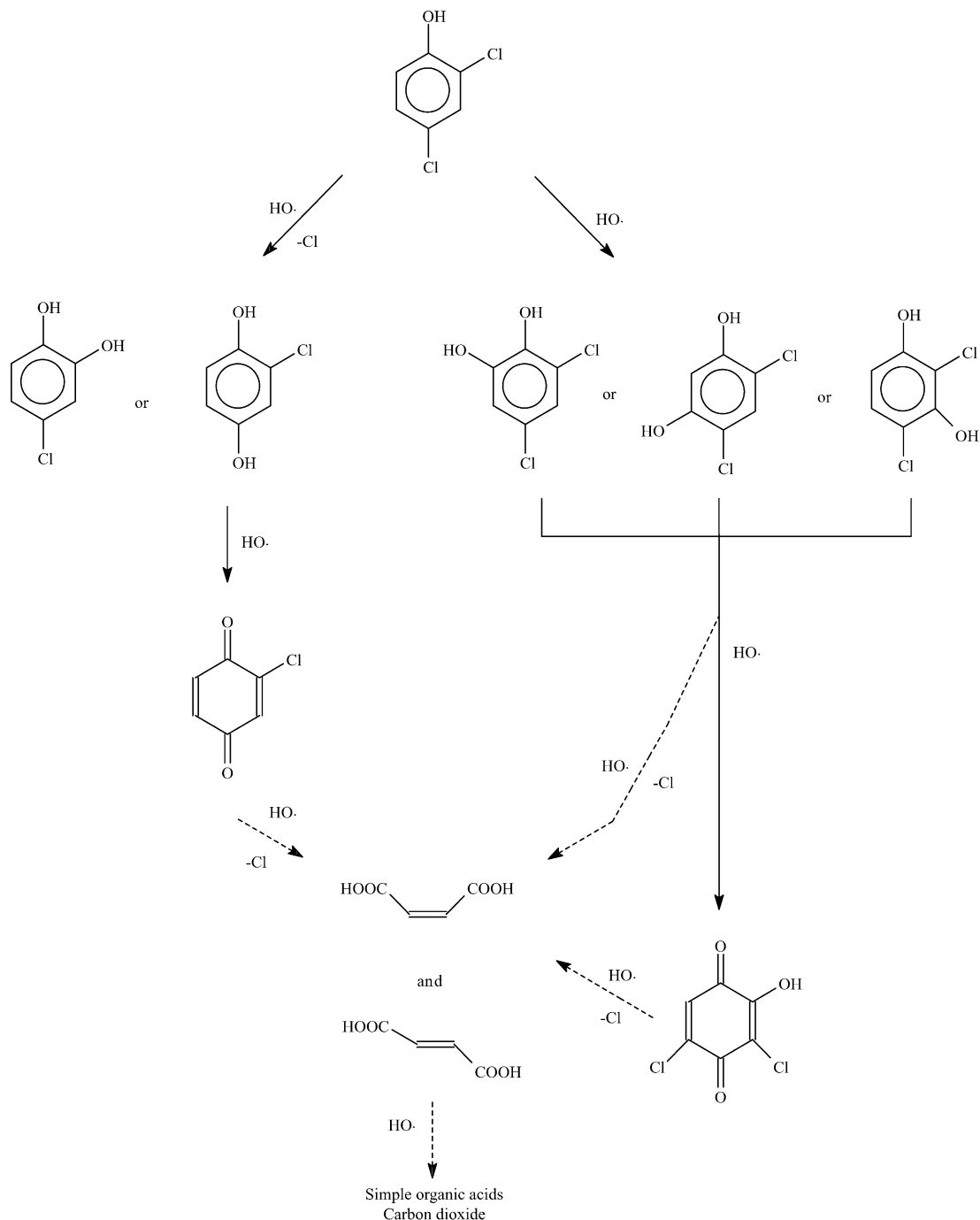


Fig. 9. Proposed reaction pathway of the photodegradation of 2,4-DCP in a photo-Fenton-like oxidation.

the FDF in practice is to increase the concentration of H_2O_2 , as a smaller $\text{Fe(III)}/\text{H}_2\text{O}_2$ ratio leads to a higher overall oxidation of 2,4-DCP.

By using the above proposed model (Eq. (11)) and the equations for the two characteristic parameters as summarized below, all of the intercepts and slope terms can be resolved using Eqs. (15)–(18):

$$\rho = \text{intercept}_\rho + \text{slope}_\rho \times [\text{Fe(III)}/\text{H}_2\text{O}_2] \quad (19)$$

$$1/\sigma = \text{intercept}_\sigma + \text{slope}_\sigma \times [\text{Fe(III)}/\text{H}_2\text{O}_2] \quad (20)$$

The consequent kinetic curve (i.e., reaction profile) at a specific reaction condition ($0.2 \text{ mM} < [\text{Fe}^{3+}] < 0.4 \text{ mM}$) can be developed for purposes of practicality. To verify the proposed model, the experimental data and modelled curves are compared in Fig. 8, where the curves show a good fit to the experimental data.

3.3. Proposed reaction mechanism

To study the intermediates of the 2,4-DCP transformation by $\text{Fe}^{3+}/\text{H}_2\text{O}_2/\text{UVC}$, the initial concentration of 2,4-DCP was elevated to 1.0 mM and irradiated in a mixture of 0.4 mM Fe^{3+} and 1.2 mM H_2O_2 at a pH level of 3.05. A reaction mechanism based on the LC/MS data was proposed in Fig. 9.

The measurable aromatic intermediates that were identified were chlorohydroquinone (CHQ), 4-chlorocatechol, 2-chloro-1,4-benzoquinone, 3,5-dichlorocatechol, 2,4-dichlororesorcinol, 4,6-dichlororesorcinol, and 3,5-dichloro-2-hydroxy-1,4-benzoquinone. It is believed that hydroxyl radicals are responsible for the transformation of 2,4-DCP by attacking 2,4-DCP in the following ways:

- By substituting an electron-withdrawing group (i.e., chlorine): The 2,4-DCP has two chlorine atoms located in the para- and ortho-positions to the aromatic ring, which were substituted by $\bullet\text{OH}$ to yield CHQ and 4-chlorocatechol, respectively.
- By the oxidation of chlorinated hydroquinone to quinone: the chlorinated hydroquinone may dissociate two hydrogen atoms to give the corresponding quinone, such as 2-chloro-1,4-benzoquinone, in response to further hydroxyl radical attacks. Given that 2-chloro-1,4-benzoquinone is the dominant quinone detectable in the solution, the para-site is apparently the preferred location for $\text{HO}\bullet$ radical attacks on the 2,4-DCP. This is likely due to the steric effect, in which the chlorine at the ortho-site is hindered by the nearby hydroxyl group compared to that at a para-site that is more approachable for radical collisions. A similar observation was also reported in the photodegradation of 2,4-D in titanium dioxide suspensions [28].
- By the addition of $\text{HO}\bullet$ to the aromatic ring: This mechanism allows an electrophilic $\text{HO}\bullet$ group to be added onto the aromatic ring of the 2,4-DCP, leading to the formation of isomers including 3,5-dichlorocatechol, 2,4-dichlororesorcinol, and 4,6-dichlororesorcinol (as indicated by three peaks exhibiting a 9:6:1 cluster at $m/z = 177$ $[\text{M} - \text{H}]^-$, 179 $[\text{M} + 2 - \text{H}]^-$, and 181 $[\text{M} + 4 - \text{H}]^-$ in the chromatograph under negative ionization). Similarly, 4,6-dichlororesorcinol was reported by Brillas et al. [29] to be the hydroxylated product of 2,4-DCP. The three isomers would then undergo further hydroxylation, but such intermediates were not detectable because they were rapidly dehydrogenated to their corresponding quinone (as detected at $m/z = 191$ $[\text{M} - \text{H}]^-$, 193 $[\text{M} + 2 - \text{H}]^-$, and 195 $[\text{M} + 4 - \text{H}]^-$ with a splitting ratio of 9:6:1, characterized by two typical $^{35}\text{Cl}/^{37}\text{Cl}$ atom clusters). The suggested structure of this compound is 3,5-dichloro-2-hydroxy-1,4-benzoquinone [30].
- By the breakdown of the aromatic ring: It was reported that hydroxyl radicals would break the aromatic rings of this chlorobenzoquinone and other hydroxylated products, resulting in maleic acids, fumaric acids, and sim-

pler organic acids (via decarboxylation), including acetic acid, formic acid, glyoxylic acid, and oxalic acid [31,32]. If there are no additional radical competitors in the solution, these low molecular organic acids can gradually be mineralized to carbon dioxide [29,33].

4. Conclusion

The decay of 2,4-DCP by a photo-Fenton-alike process was studied under various conditions: $0.1 \leq [\text{Fe}^{3+}] \leq 0.4$ mM, $0.05 \leq [\text{H}_2\text{O}_2] \leq 2.0$ mM, and $0.20 \leq \text{Fe(III)}/\text{H}_2\text{O}_2 \leq 2.00$. As the initial concentration of Fe^{3+} was low (i.e., 0.1 mM), the decay followed a pseudo first-order kinetic. However, as $[\text{Fe}^{3+}]$ was increased to higher levels, it was interesting to note that the oxidation process no longer followed the simple pseudo first-order kinetics. As a result, a mathematic model was developed to predict such a non-conventional kinetic process. Through the use of the proposed model, the photo-Fenton-like process can be described using two character parameters: the initial decay rate ($1/\rho$) and the final decay fraction ($1/\sigma$). It was found that the model can successfully predict the kinetic curves of the 2,4-DCP decay within the tested ranges, which could be helpful in optimizing predictions of the use and performance of $[\text{Fe}^{3+}]$ and $[\text{H}_2\text{O}_2]$ in a treatment work design. The reaction intermediates in $\text{Fe}^{3+}/\text{H}_2\text{O}_2/\text{UVC}$ system were identified and the associated reaction mechanisms were proposed and discussed.

References

- M.A. Crespín, M. Gallego, M. Valcárcel, *Environ. Sci. Technol.* 35 (2001) 4265.
- A. Laganà, A. Bacaloni, I. De Leva, A. Faberi, G. Fago, A. Marino, *Anal. Chim. Acta* 462 (2002) 187.
- D.E. Barnekow, N.D. Premkumar, S. Stewart, A.W. Hamburg, *J. Agric. Food Chem.* 49 (2001) 2853.
- F. Laurent, L. Debrauwer, E. Rathahao, R. Scalla, *J. Agric. Food Chem.* 48 (2000) 5307.
- B.B. Sithole, D.T. Williams, *Assoc. Off. Anal. Chem.* 69 (1986) 807.
- N.V. Heeb, I.S. Dolezal, T. Bühner, P. Mattrel, M. Wolfensberger, *Chemosphere* 31 (1995) 3033.
- M. Pérez, F. Torrades, J.A. García-Hortal, X. Domènech, J. Peral, *Appl. Catal. B: Environ.* 36 (2002) 63.
- T.K. Boucard, R.D. Bardgett, K.C. Jones, K.T. Semple, *Environ. Pollut.* 133 (2005) 53.
- A.A.M. Daifullah, B.S. Girgis, *Water Res.* 32 (1998) 1169.
- N. Calace, E. Nardi, B.M. Petronio, M. Pietroletti, *Environ. Pollut.* 118 (2002) 315.
- L. Jakob, T.M. Hashem, S. Bürki, M.N. Guindy, A.M. Braun, *J. Photochem. Photobiol. A* 75 (1993) 97.
- P. Piccinini, P. Pichat, C. Guillard, *J. Photochem. Photobiol. A* 119 (1998) 137.
- N.J. Bunce, Y. Kumar, S. Safe, *J. Chem. Soc., Perkin Trans. 2* (1978) 880.
- H.D. Burrows, L.M. Canle, J.A. Santaballa, S. Steenken, *J. Photochem. Photobiol. B* 67 (2002) 71.
- A. Hirvonen, P. Kalliokoski, T. Tuhkanen, *Water Sci. Technol.* 33 (1996) 67.

- [16] W.S. Kuo, Chemosphere 39 (1999) 1853.
- [17] W. Chu, Chemosphere 44 (2001) 935.
- [18] C.Y. Kwan, W. Chu, Water Res. 37 (2003) 4405.
- [19] M. Pera-Titus, V. García-Molina, M.A. Baños, J. Giménez, S. Esplugas, Appl. Catal. B: Environ. 47 (2004) 219.
- [20] M. Kositzki, I. Poullos, S. Malato, J. Caceres, A. Campos, Water Res. 38 (2004) 1147.
- [21] M. Rodríguez, V. Sarria, S. Esplugas, C. Pulgarin, J. Photochem. Photobiol. A 151 (2002) 129.
- [22] M. Neamtu, A. Yediler, I. Siminiceanu, A. Kettrup, J. Photochem. Photobiol. A 161 (2003) 87.
- [23] I. Arslan-Alaton, F. Gurses, J. Photochem. Photobiol. A 165 (2004) 165.
- [24] M.A. Engwall, J.J. Pignatello, D. Grasso, Water Res. 33 (1999) 1151.
- [25] G. Ghiselli, W.F. Jardim, M.I. Litter, H.D. Mansilla, J. Photochem. Photobiol. A 167 (2004) 59.
- [26] H. Gallard, J. De Laat, B. Legube, Water Res. 33 (1999) 2929.
- [27] K.H. Chan, W. Chu, Water Res. 37 (2003) 3997.
- [28] J.C. D'Oliveira, C. Minero, E. Pelizzetti, P. Pichat, J. Photochem. Photobiol. A: Chem. 72 (1993) 261.
- [29] E. Brillas, J.C. Calpe, J. Casado, Water Res. 34 (2000) 2253.
- [30] A. Lopez, G. Mascolo, A. Detomaso, G. Lovecchio, R. Ciannarella, R. Curci, Proceedings of the 3rd International Conference on Oxidation Technologies for Water and Wastewater Treatment, CUTEC, Germany, 2003, p. 470.
- [31] R. Zona, S. Solar, P. Gehringer, Water Res. 36 (2002) 1369.
- [32] E. Brillas, J.C. Calpe, P.-L. Cabot, Appl. Catal. B: Environ. 46 (2003) 381.
- [33] C. Comninellis, A. Nerini, J. Appl. Electrochem. 25 (1995) 23.